Effectof the particlesize distributiononthe heattransfermechanismsandthe heatstoragecapacityin ceramic inserts made by alkaline activation.

Keywords: ceramic insert, improved hearth, geopolymers, alkali-activation, environment, thermal behaviour, combustion, particle size analysis, microstructure, storage capacity, thermal tests

1. Introduction

The market for ceramic inserts is experiencing a significant growth. This is due to the fact that ceramic inserts are very economical in relation to the amount of charcoal, which further contributes to the decline in deforestation. However, it should be noted that during and after their manufacture, many problems arise, in particular the losses of inserts due to their fragility, their low performance and the lack of energy for cooking. These shortcomings testify to the need to move towards other, more productive alternatives to strengthen the fight against deforestation. Moreover, the development of the science of geopolymers based on the reaction of an aluminosilicate with an alkaline, sodium or potassium solution and applicable in several fields seemed to us to be an excellent asset in improving their performance, increasing their resistance and reducing the cooking energy. Geopolymerization and alkaline activation of aluminosilicates constitute a possible alternative to meet these technical and environmental challenges [1]. This involves the exploitation of co-products from other industries (fly ash, blast furnace slag, etc.) and materials with a low environmental impact (metakaolin, pozzolans) [2], the implementation of these new materials is now being realized around the world through various and innovative applications. In addition to concrete and building materials, their properties make them suitable for use in thermal insulation, aeronautics, ceramics, coatings, etc. After discreet beginnings in the 70s and 80s, research around alkali-activated geopolymers and binders is accelerating steadily, leading to a better knowledge of the specificities of their manufacture and use [3, 4].The number of theses, articles and patents attests to the growing interest in these materials among researchers as well as industrialists, which makes it possible to predict a promising market for the coming years [5,6] Great importance has therefore been reserved for the characterization of the raw materials and for understanding their influence on the reaction mechanisms and the structuring of the cured material by focusing on degradation by exposure to drying, the performance of selected formulations is compared with existing inserts according to different indicators. The objective is to define the main degradation mechanisms present and to allow the designation of the most suitable compositions according to the conditions of use.

2.Materials and Methods

2.2 Presentation of Thiéky clays

The Thiéky clay deposit is in the Ndiass horst, 4 km south of the Dakar-Kaolack National Road. Between Sindia and Popenguine [7], an area of clay hills extends from Thiéky to this road. The Thiéky sector belongs to the Maastrichtian age formations of the Ndiass horst which constitutes the eastern part of the Cape Verde peninsula. These are sandstone, clayey formations with some sandy and lateritic pasts. These formations of the Cape Verde peninsula are also found in the western part of the Senegalo-Mauritanian basin whose base sinks slightly from East to West to a depth of 6000 m vertically Dakar.

2.3 Presentation of Sebikhotane clays

It is a gray clay forming a thin veneer, with a fairly significant extension in the direction of Lake Tamna. In Sébikhotane, clay appears between the national road and the railway. It is used by a small artisanal brick and pottery factory. In Gandoul, gray-colored clay has been extensively prospected with a view to a cement plant. At first glance, the reserves are quite large, but their exploitation could possibly interfere with the Gandoul radio-satellite antenna. The Sebikhotane deposit consists of two layers of clay: a surface layer of gray blue color and a lower layer of yellow color. Preliminary tests have provided the following results :

- ❖ The surface layer
- Vintageappearance: gray, blackish, semi-oily
- Drying shrinkage : 4.5 %
- Cookingtime : 7 %
- Bakedappearance : brick red, orange
- Weight of water absorbed : 16.4 g
- Workability : very good
- Observation : can be worked directly
- ❖ The bottom layer
- Vintageappearance : very dark brown
- Dryingshrinkage : 7 %
- Cookingtime : 1 %
- Bakedappearance : dark red
- Weight of water absorbed : 12 g
- Workability : very good

- Observation : can be worked directly

2.4 Presentation of Paki-Toglou

Cranes These are the Maastrichtian sandstones, sub-outcrops in the Ndiass massif where they are covered by lateritic formations whose power can exceed 10 m. The Paki-Toglou deposit, which includes almost all the sandstone operations, is located at 50 km from Dakar to the West of Paki village, on the road to Diamniadio Mbour. The material is a pinkish sandstone with siliceous cement and fine grains. The standard Deval tests carried out on samples taken at the level of the hill of Paki gave the results which are recorded in Table I

Table 1: Results of the Deval Standard tests.

Place of collection	**Standard Deval Coefficient**
Hillside	2,2
Hillside	9,7
Hillside well	16,6
Well at the top of the hill	12,5
Well at the top of the hill	8,9

These results show the heterogeneity of the deposit which is represented by an alternation of hard banks and soft banks. "**LALEYE, 1965"** has carried out several wells which have made it possible to estimate very approximately the reserves of the Paki sandstone deposits.

Table 2:The reserves of the Paki sandstone deposits

Paki deposit	300000 t
Toglou deposit	150000 t
Mbang deposit	3000000 t
Total	3450000 t

2.5 Implementation of solutions

During our experiment, we used sodium hydroxide as an activator in the form of a 98% pure solid grain. The reason for our choice, beyond the fact that sodium is an alkali metal, is its

availability on the market, its low cost and its reactivity. Sodium hydroxide in different masses is mixed with distilled water to obtain solutions of different concentrations:

- ❖ Formula C1 for the solution of molar concentration= 2 moles or 80 g NaOH/ liter of solution.
- ❖ Formula C2 for the solution of molar concentration= 6 moles or 240 g NaOH/ liter of solution.

For the two solutions we used the same amount of distilled water of 10 liters. The distilled water makes it possible to preserve the purity of the reaction and the mass of sodium hydroxide is determined from the formula below:

$$m_i = C_i . M_i . V$$

With m_i= mass of sodium hydroxide of the solution C_i (i= 1, 2) (in grams); C= desired NaOH concentration (mol/liters); M =molecular molar mass of sodium hydroxide (40 g/mol) and V volume of distilled water (10 liters) Which allows us to obtain $m_1 = 800g$, and $m_2 = 24000g$ [8].

2.6 Implementation of ceramic inserts

To make our inserts, we chose the one that weighs 4600 g for the manufacture of the Jambar stove [9].

Thus, we have:

- 50% of Sebikhotane clays.
- 30% of Thiéky clays.
- 20% of Toglou stoneware, it facilitates the recovery of the insert in the mold.

For the Sebikhotane clays, we used the 500-micron sieve passers and the same particle size for the Thiéky clays;however, for the Toglou sandstones, the 1600-micron sieve passers are used. The choice of particle size is very important and allows us to standardize our materials well.

After this step, the implementation consists in using the caustic solution as wetting water based on the results of the Proctor test [10]. Indeed, on the one hand it required a certain amount of alkaline solution to reach the reaction of formation of the geopolymers and on the other hand it was imperative not to exceed the Proctor optimum of our material because the caustic solution is obtained from water.

In total we have made 10 inserts including 5 inserts for each solution and each weigh 4600 g.

Table 3 : Summary of the mixing volumes and the quantities of materials used for the insert the values will thus be presented in the table

	Solution C1	**Solution C2**
Volume used for the 5 inserts in liters	**12,25**	**14,4**
Quantity used for the 5 g inserts	**23000**	**23000**

2.7 Description of the Laser granulometer

2.7.1. Objective

The particle size distribution is deduced from the interaction between a set of particles and the incident laser beam by analyzing the beam diffraction spot with 2 dispersion modes: dry or wet

2.7.2. Principle: international standard ISO 13320

The Cilas 990 is a particle size analyser based on laser diffraction (laser diffraction). This principle is based on the diffraction of light by the particles:

- A laser beam passes through a cloud of scattered particles.
- The particles deflect (diffraction) the light at different angles depending on their size.
- A detector measures the intensity of the diffracted light at various angles.
- A software converts these signals into a distribution of particle sizes by volume or number, often expressed by statistical values such as D10, D50, D90.

This principle is based on the theories of Mie and Fraunhofer, which make it possible to model the laser diffraction mathematically according to the size of the particles

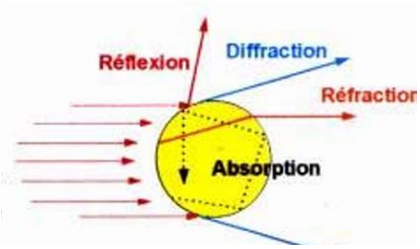

Figure 1: Interaction between incident light and Particle

A laser granulometer typically consists of five subsets:

- A powder dispersion system
- A system for circulating the powder
- An electronic assembly for amplifying the measurement signals an optical bench a microcomputer

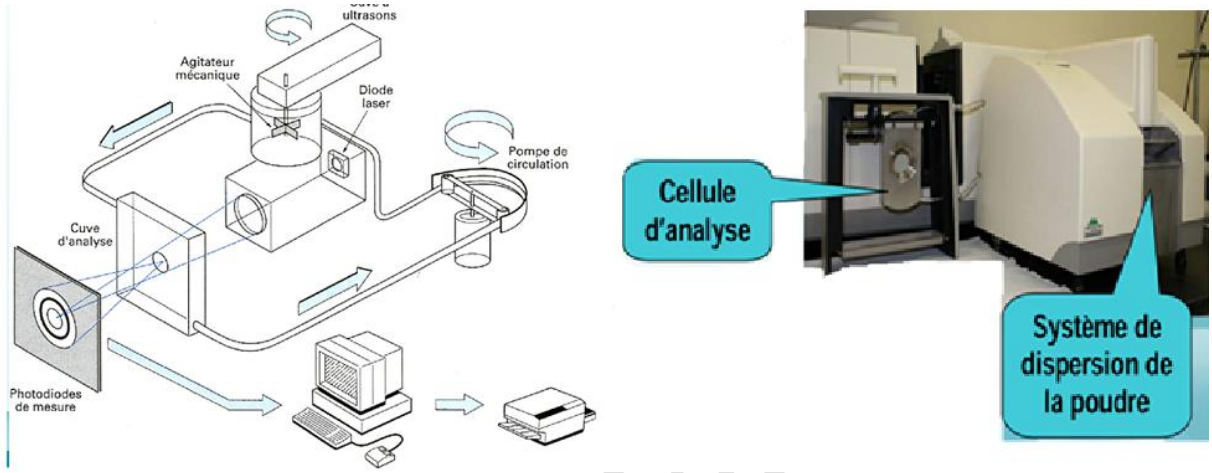

Figure 2: Devices and system for analysing the Laser granulometer

3.Results and discussion

3.1. Particle size analysis of Sebikhotane clays

The figure 1shows the particle size distribution of the sebikhotane clays produced on a laser analyzer. The histogram of the particle size distribution of the Sebikhotane clays highlights a distribution dominated by fine fractions (clays < 2 µm) characteristic of clayey materials rich in phyllosilicate minerals, with a secondary proportion of fine silts, reflecting an overall very fine texture and a high specific surface area ; this particle size organization is closely linked to the thermal behavior of the material, because the increase in temperature induces progressive physico-chemical transformations which preferably affect the finest particles. Indeed, at low temperatures (≤ 100-200 ° C.), the elimination of adsorbed and interfoliar water occurs without major modification of the apparent distribution, while at intermediate temperatures (400-700 ° C.), the dehydroxylation of clay minerals (in particular kaolinite and illite) favors the agglomeration of fine particles, which may result in a relative displacement of the particle size classes towards coarser sizes on the histogram ; at higher temperatures (>800-900 °C), the phenomena of sintering and vitrification reinforce this tendency, reducing the ultrafine fraction and increasing the structural cohesion of the material. Thus, the observed particle size distribution constitutes a relevant indicator of the thermal sensitivity of Sebikhotane clays and

their suitability for uses requiring mechanical and thermal stability, such as ceramics or building materials, in accordance with observations widely reported in the literature on the thermal behavior of natural clays [11].

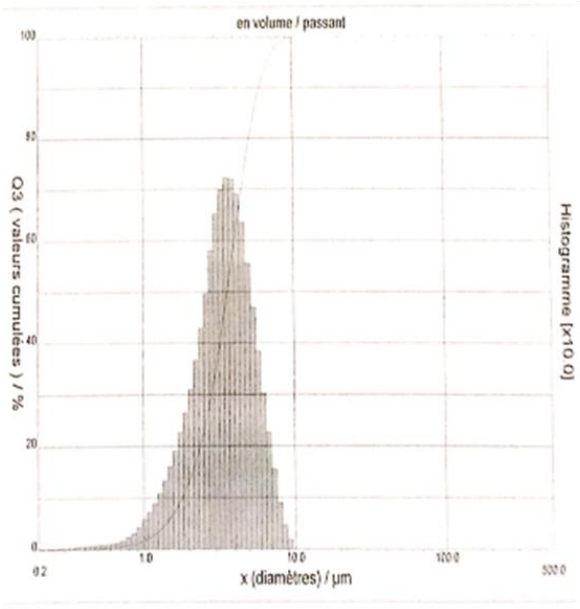

Valeurs cumulées caractéristiques — en volume / passant

x	0.20	0.30	0.40	0.50	0.60	0.70	0.80	0.90	1.00	1.10
Q3	0.00	0.04	0.15	0.32	0.51	0.71	0.95	1.29	1.76	2.39
q3	0.00	0.01	0.04	0.07	0.10	0.12	0.17	0.27	0.42	0.62
x	1.20	1.30	1.40	1.50	1.80	2.00	2.20	3.40	3.60	3.80
Q3	3.15	4.03	5.02	7.36	10.13	13.28	16.77	20.64	24.88	34.21
q3	0.82	1.03	1.25	1.64	2.20	2.79	3.42	4.15	4.92	6.10
x	3.20	3.60	4.00	4.30	4.60	5.00	5.60	6.00	6.50	7.00
Q3	39.33	49.62	59.33	65.92	71.81	78.49	86.05	89.78	93.27	95.77
q3	7.40	8.15	8.60	8.50	8.15	7.48	6.23	5.05	4.07	3.15
x	8.00	9.00	10.00	11.00	12.00	13.00	14.00	15.00	17.00	20.00
Q3	98.53	99.69	100.00	100.00	100.00	100.00	100.00	100.00	100.00	100.00
q3	2.00	0.64	0.27	0.00	0.00	0.00	0.00	0.00	0.00	0.00
x	22.00	25.00	28.00	32.00	36.00	40.00	45.00	50.00	56.00	63.00
Q3	100.00	100.00	100.00	100.00	100.00	100.00	100.00	100.00	100.00	100.00
q3	0.00	0.00	0.00	0.00	0.00	0.00	0.00	0.00	0.00	0.00
x	66.00	71.00	75.00	80.00	85.00	90.00	100.0	112.0	140.0	160.0
Q3	100.00	100.00	100.00	100.00	100.00	100.00	100.00	100.00	100.00	100.00
q3	0.00	0.00	0.00	0.00	0.00	0.00	0.00	0.00	0.00	0.00
x	180.0	200.0	224.0	250.0	280.0	315.0	355.0	400.0	450.0	500.0
Q3	100.00	100.00	100.00	100.00	100.00	100.00	100.00	100.00	100.00	100.00
q3	0.00	0.00	0.00	0.00	0.00	0.00	0.00	0.00	0.00	0.00

x : diamètres / µm Q3 : cumulé / % q3 : densité population

Fig3: Particle size analysis of Sebikhotane clays

3.2. Particle size analysis of Thiéky clays

The figure 2 shows the particle size distribution of the Thiéky clays produced on a laser analyzer. The histogram of the particle size distribution of Thiéky clays highlights a marked dominance of fine fractions (clays < 2 µm), associated with a secondary proportion of silts, which reflects a highly plastic material rich in clay minerals. This fine particle size distribution is decisive for the thermal behavior of the clay : when the temperature rises, the high specific surface area of the fine particles first favors the loss of adsorbed and interfoliar water at low temperature (< 200 ° C.), then the progressive dehydroxylation of the clay minerals (in particular kaolinite and / or illites) between 400 and 700 ° C., resulting in an irreversible modification of the crystalline structure. At higher temperatures (> 800 ° C.), the predominance of fine fractions accentuates the phenomena of sintering and vitrification, leading to a reduction in porosity and an increase in the density and mechanical strength of the material, unlike coarser materials which require higher temperatures to reach a state comparable. Thus, the relationship highlighted by the histogram between fine particle size and temperature confirms that Thiéky clays have a high thermal sensitivity, with a behavior adapted to ceramic uses or construction materials fired at moderate temperature, which is

consistent with the classical models linking particle size fineness, thermal transformations and final properties of clays [12].

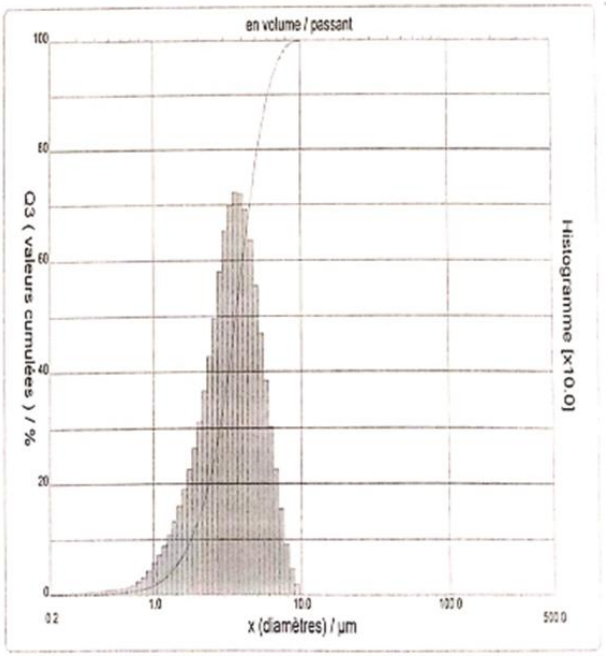

Valeurs cumulées caractéristiques — en volume / passant

x	0.20	0.30	0.40	0.50	0.60	0.70	0.80	0.90	1.00	1.10
Q3	0.00	0.04	0.15	0.32	0.51	0.71	0.95	1.29	1.76	2.39
q3	0.00	0.01	0.04	0.07	0.10	0.12	0.17	0.27	0.42	0.62
x	1.20	1.30	1.40	1.60	1.80	2.00	2.20	2.40	2.60	3.00
Q3	3.15	4.03	5.02	7.36	10.13	13.28	16.77	20.64	24.86	34.21
q3	0.82	1.03	1.25	1.64	2.20	2.79	3.42	4.15	4.92	6.10
x	3.20	3.60	4.00	4.30	4.60	5.00	5.60	6.00	6.50	7.00
Q3	39.33	49.62	59.33	65.92	71.81	78.49	86.05	89.78	93.27	95.77
q3	7.40	8.15	8.60	8.50	8.15	7.48	6.23	5.05	4.07	3.15
x	8.00	9.00	10.00	11.00	12.00	13.00	14.00	15.00	17.00	20.00
Q3	98.63	99.69	100.00	100.00	100.00	100.00	100.00	100.00	100.00	100.00
q3	2.00	0.84	0.27	0.00	0.00	0.00	0.00	0.00	0.00	0.00
x	22.00	25.00	28.00	32.00	36.00	40.00	45.00	50.00	56.00	63.00
Q3	100.00	100.00	100.00	100.00	100.00	100.00	100.00	100.00	100.00	100.00
q3	0.00	0.00	0.00	0.00	0.00	0.00	0.00	0.00	0.00	0.00
x	66.00	71.00	75.00	80.00	85.00	90.00	100.0	112.0	140.0	160.0
Q3	100.00	100.00	100.00	100.00	100.00	100.00	100.00	100.00	100.00	100.00
q3	0.00	0.00	0.00	0.00	0.00	0.00	0.00	0.00	0.00	0.00
x	180.0	200.0	224.0	250.0	280.0	315.0	355.0	400.0	450.0	500.0
Q3	100.00	100.00	100.00	100.00	100.00	100.00	100.00	100.00	100.00	100.00
q3	0.00	0.00	0.00	0.00	0.00	0.00	0.00	0.00	0.00	0.00

x : diamètres / µm Q3 : cumulé / % q3 : densité population

Fig4: Particle size analysis of Thiéky clays

3. 3. Particle size analysis of Paki-Toglou Sandstone

The figure 3 shows the particle size distribution of the sebikhotane clays produced on a laser analyzer.

The histogram of granulometric distribution of the Paki-Toglou sandstones highlights a dominance of medium to coarse sandy fractions, reflecting a relatively good sorting and a high deposition energy, characteristics of a sedimentary environment with sustained dynamics, such as a fluvial or shallow coastal context; this distribution suggests that the initial texture of the sandstone strongly determines its subsequent thermal response, because the size and organization of the grains control both the intergranular porosity and the thermal conductivity of the material. Indeed, when the temperature increases, in particular under conditions of thermal diagenesis or experimental heat treatments, sandstones with a coarser and better sorted particle size generally exhibit better heat diffusion, limiting the internal thermal gradients, while the differential expansion of the quartz grains and the cements can induce progressive microcracks, affecting the mechanical cohesion and the physical properties of the rock. Thus, the observed relationship between the dominant grain size of the Paki-Toglou sandstones and the temperature reflects a texture thermal behavior coupling, where a relatively homogeneous sandy grain size favors a more stable thermal response at low and

medium temperature, but can become a weakening factor at high temperature by accumulation of thermal stresses at grain-grain contacts [20].

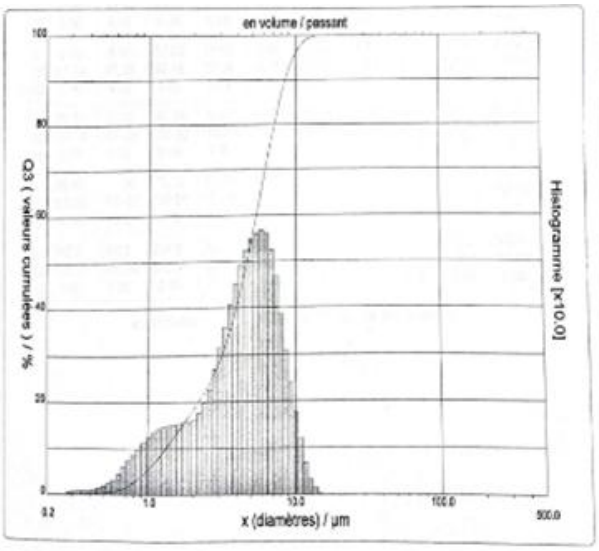

Valeurs cumulées caractéristiques — en volume / passant

x	0.20	0.30	0.40	0.50	0.60	0.70	0.80	0.90	1.00	1.10
Q3	0.00	0.00	0.23	0.47	0.93	1.66	2.77	4.04	5.43	6.88
q3	0.00	0.00	0.08	0.10	0.24	0.45	0.79	1.02	1.25	1.44
x	1.20	1.30	1.40	1.60	1.80	2.00	2.20	2.40	2.60	3.00
Q3	8.34	9.77	11.14	13.67	15.95	18.04	19.95	21.84	23.80	26.06
q3	1.59	1.69	1.75	1.80	1.84	1.88	1.90	2.06	2.32	2.82
x	3.20	3.60	4.00	4.30	4.60	5.00	5.60	6.00	6.50	7.00
Q3	30.48	35.65	41.16	45.42	49.69	55.28	63.26	68.20	74.00	79.15
q3	3.56	4.16	4.96	5.59	6.00	6.35	6.68	6.79	6.87	6.59
x	8.00	9.00	10.00	11.00	12.00	13.00	14.00	15.00	17.00	20.00
Q3	87.29	92.58	95.94	97.98	99.15	99.68	99.91	100.00	100.00	100.00
q3	5.78	4.26	3.02	2.03	1.28	0.63	0.29	0.12	0.00	0.00
x	22.00	25.00	28.00	32.00	35.00	40.00	45.00	50.00	56.00	63.00
Q3	100.00	100.00	100.00	100.00	100.00	100.00	100.00	100.00	100.00	100.00
q3	0.00	0.00	0.00	0.00	0.00	0.00	0.00	0.00	0.00	0.00
x	66.00	71.00	75.00	80.00	85.00	90.00	100.0	112.0	140.0	160.0
Q3	100.00	100.00	100.00	100.00	100.00	100.00	100.00	100.00	100.00	100.00
q3	0.00	0.00	0.00	0.00	0.00	0.00	0.00	0.00	0.00	0.00
x	180.0	200.0	224.0	250.0	280.0	315.0	355.0	400.0	450.0	500.0
Q3	100.00	100.00	100.00	100.00	100.00	100.00	100.00	100.00	100.00	100.00
q3	0.00	0.00	0.00	0.00	0.00	0.00	0.00	0.00	0.00	0.00

x : diamètres / µm Q3 : cumulé / % q3 : densité population

Fig 5: Particle size analysis of the Paki-Toglou Sandstone

3. 4. Evaluation of the heat absorption and restitution potential of the inserts

The objective of this test is to evaluate the potential for absorption, storage and restitution of the heat of the inserts through the water boiling test [13] by analyzing the evolution of the temperature of the water and of the insert stove system during the heating and cooling phases. This test makes it possible to quantify the ability of the inserts to absorb the thermal energy produced, to conserve it [14], then to restore it in a delayed manner, highlighting their thermal efficiency, their thermal inertia and their contribution to improving energy efficiency and reducing heat losses in clean cooking applications. The potential of absorption and restitution of the heat of the inserts was evaluated using the boiling water test [15].

The evaluation of the absorption, storage and heat recovery potential of the inserts was carried out using the boiling water test, a method widely used for the characterization of the thermal performance of cooking systems and materials with high thermal inertia. The experimental protocol was structured in two successive phases: a heating phase and a controlled cooling phase.

The heating phase consists of placing the insert inside the stove, subjected to active combustion for a period of 30 minutes. A container containing a mass of water initially at room temperature is positioned above the hearth. The water temperature is measured at regular intervals using a calibrated thermometer, making it possible to follow the kinetics of temperature rise. This phase aims to evaluate the ability of the insert to absorb the thermal

energy produced, to transfer it to the container and to contribute to the rise in the temperature of the water, a direct indicator of the efficiency of the heat transfer of the system.

At the end of the heating phase, the combustion is interrupted by the complete emptying of the stove, in order to eliminate any active source of heat. The system is then left in natural cooling for a period of 1 hour, without additional energy input. During this phase, the evolution of the temperature of the water and or of the insert is recorded in order to analyze the progressive restitution of the stored heat. The observed thermal decrease makes it possible to characterize the thermal inertia of the insert, as well as its ability to restore the stored energy after the combustion has stopped. The joint analysis of the data from the heating and cooling phases thus makes it possible to quantify the overall thermal behavior of the inserts, in particular their suitability for thermal storage and their potential contribution to improving energy efficiency and reducing heat losses in clean cooking systems.

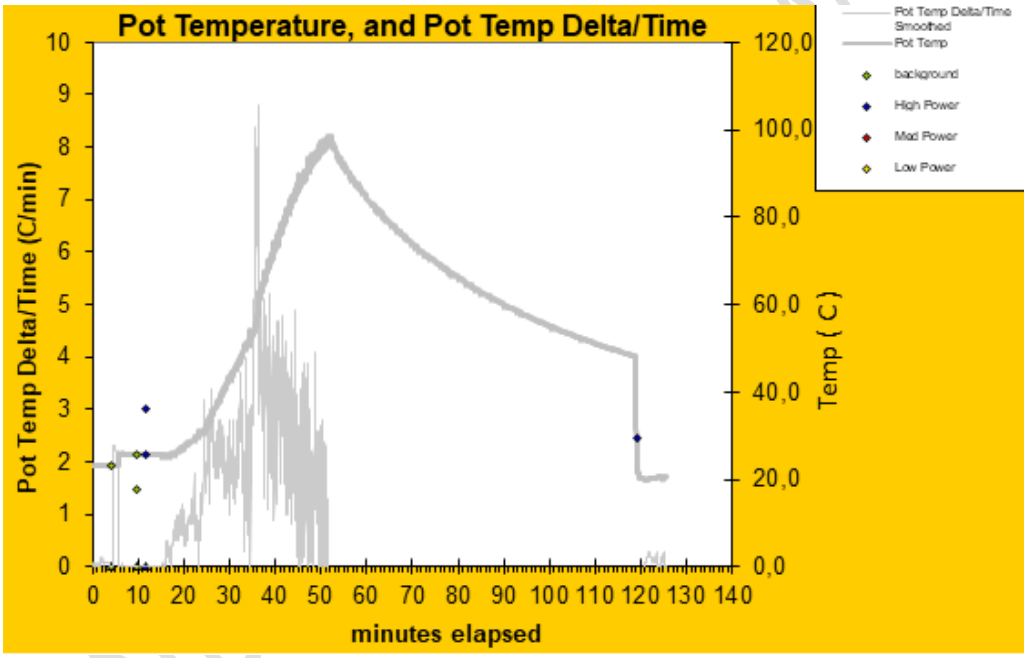

Fig 6: Temperature variation curve for C1

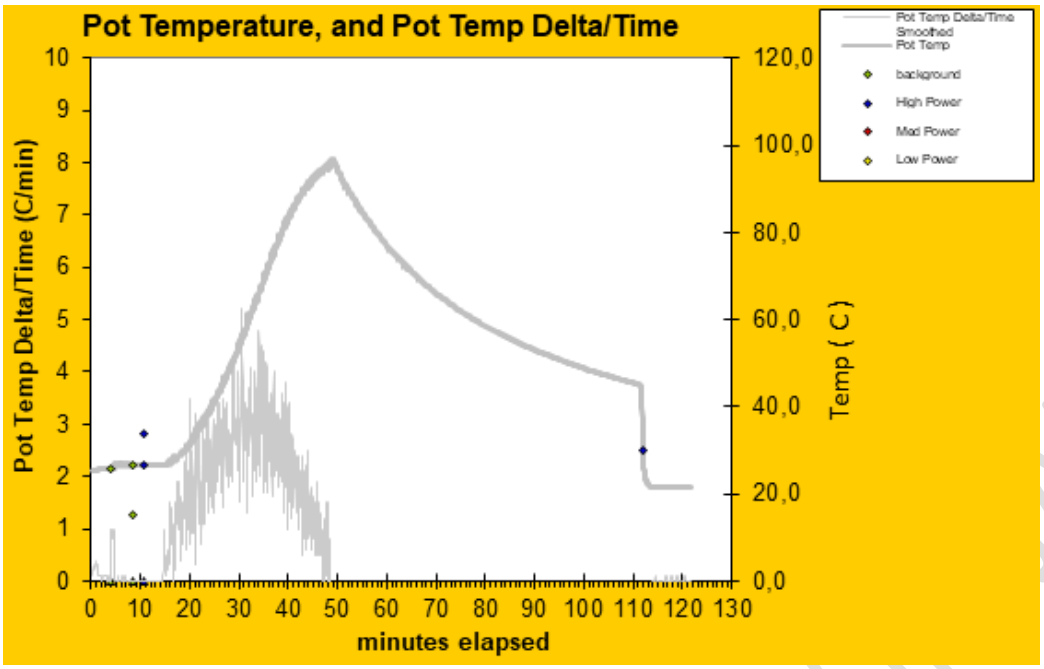

Fig 7 : Temperature variation curve for C2

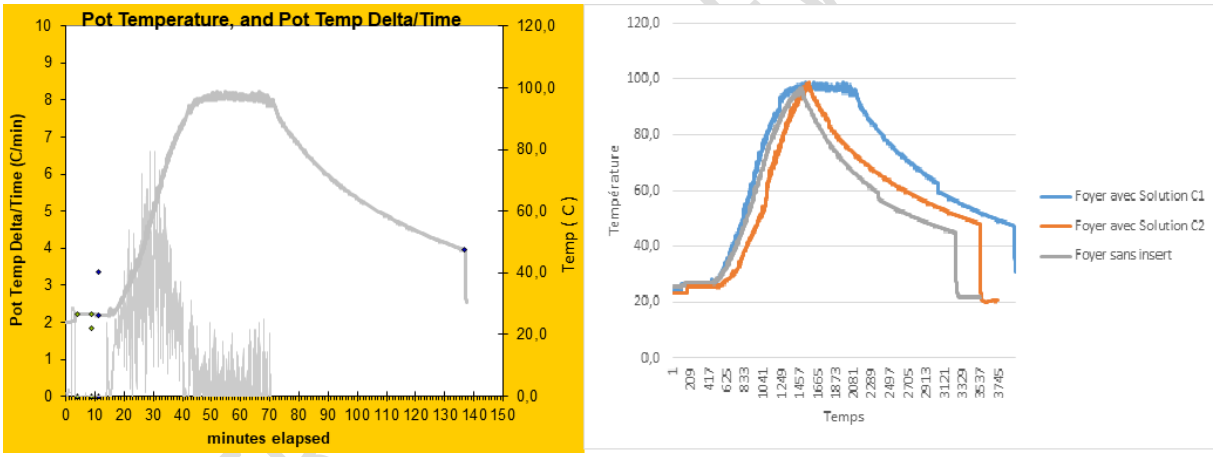

a) for fireplace without insert b) for C1, C2 and Fireplace without insert

Figure 8: Curve of variation of the temperature as a function of time

The temperature curves as a function of time highlight the compared thermal behavior of three stoveconfigurations: a stove without insert, a stove equipped with the C1 solution and a stove equipped with the C2 solution. Overall, the three systems have a similar thermal dynamic characterized by a rapid temperature rise phase, a plateau close to the maximum temperature, then a decrease phase corresponding to the cooling of the system after extinction or reduction of the source of chaleur. La heating phase shows a gradual increase in temperature up to a maximum close to 95-100 ° C. However, the stove with the C1 solution

reaches this maximum more quickly and maintains a longer thermal plateau than the other two configurations. This behavior reflects a better heat absorption and redistribution capacity, generally associated with a higher thermal mass and with an adapted thermal conductivity of the ceramic insert. Conversely, the stove without insert has a slightly less efficient rise and an earlier onset of decay, suggesting greater heat losses to the environment. During the cooling phase, the differences between the systems become more marked. The stove without inserts cools quickly, with a sudden drop in temperature, which indicates a low thermal retention capacity and limited thermal inertia. The stove equipped with the C2 solution shows a moderate improvement, with a more gradual decrease, reflecting a partial retention of heat. On the other hand, the C1 solution has the lowest cooling slope and retains high temperatures for a longer period, which testifies to a higher thermal inertia and a better thermal storage efficiency. These results confirm that the integration of ceramic inserts significantly improves the thermal behavior of the fireplaces, in particular in terms of temperature stabilization and prolongation of heat recovery after the combustion phase. The C1 solution thus appears as the most efficient configuration, optimizing both the temperature rise and the thermal retention capacity. This behavior is consistent with previous work showing that increasing the thermal mass and optimizing the thermophysical properties of materials (conductivity, heat capacity) make it possible to reduce energy losses and improve the overall efficiency of improved stoves intended for domestic cooking

3.5. Combustion test results

The objective of this test is to evaluate the thermal behavior of ceramic inserts as well as their energy performance, in particular their ability to reduce solid fuel consumption [16].This approach makes it possible to determine whether the inserts optimize the heat transfer while minimizing the amount of charcoal necessary to maintain a stable temperature [17].To do this, each insert was carefully weighed in order to determine its initial weight, in accordance with standard protocols for characterizing thermal cooking devices. Subsequently, a constant quantity of charcoal of 1 kg was deposited on each insert in order to ensure the reproducibility of the tests. The fuel was then ignited, and the following measurements were carried out at regular intervals:

- Temperature of the insert, making it possible to evaluate its storage and heat recovery capacity.
- Temperature of the metal casing, in order to study the thermal losses towards the outside.

- Total weight of the fireplace plus charcoal, in order to quantify the decrease in fuel over time and to estimate the energy efficiency of the insert.

This methodology makes it possible to establish a correlation between the particle size distribution of the constituent materials of the insert, their thermal behavior and energy consumption, thus offering indications on the optimization of ceramic inserts for domestic or industrial applications

The results of Table 4 were noted every 30 minutes.

Table 4: Results of the combustion tests

	Insert of the C1 solution	Insert of the C2 solution	Insert Reference
Initial weight: insert+ charcoal	10,42 kg	10,26 kg	10,30 kg
Envelope temperature	26 °C	26 °C	26 °C
Insert temperature	26 °C	26 °C	26 °C
Weight after 30 minutes	10,40 kg	10,10 kg	9,9 kg
Envelope temperature	30,6 °C	31,1 °C	33,4 °C
Insert temperature	46,6 °C	46,1 °C	52 °C
Weight after 1 hour	9,75kg	9,68 kg	9,4 kg
Envelope temperature	109,5 °C	103,1°C	111,9 °C
Insert temperature	202,6 °C	172,9 °C	204 °C
Weight after 1h30mn	9,47 kg	9,4 kg	9,34 kg
Envelope temperature	114,6 °C	112,2 °C	110 °C
Insert temperature	233,2 °C	212 °C	224, 3 °C
Weight after 2 hours	9,4 kg	9,26 kg	9,30 kg
Envelope temperature	121 °C	119,6 °C	116,5 °C
Insert temperature	241 °C	214,3 °C	231,2 °C
Weight after emptying the insert	9,14 kg	8,96 kg	9,013 kg
Insert temperature	430 °C	445 °C	386 °C
Insert temperature 5 minutes after emptying	299 °C	310 °C	273 °C

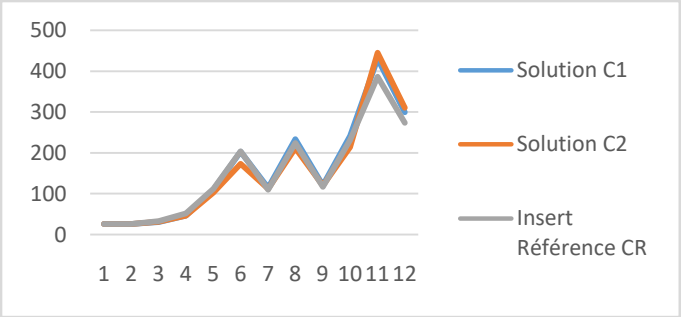

Fig 9 : Curve of variation of the temperature as a function of time

The curves C 1, C 2 and CR present a globally similar thermal evolution, characterized by three distinct phases : an initial phase of gradual temperature rise, a rapid rise phase leading to a thermal peak, then a decrease phase. During the first phase (0 to approximately 0.5 h), the temperature increases slightly for all the samples, reflecting an initial thermal inertia linked to the progressive absorption of thermal energy and to the calorific capacity of the materials. Between 0.5 h and 2 h, a more marked increase is observed, with a relatively comparable slope for the three curves, indicating a quasi-stationary heating regime dominated by the heat conduction and accumulation mechanisms. However, slight differences appear : the C1 sample has slightly higher temperatures than those of C2 and CR, suggesting a Fig7 : Curve of variation of the temperature as a function of time

The curves C 1, C 2 and CR present a globally similar thermal evolution, characterized by three distinct phases : an initial phase of gradual temperature rise, a rapid rise phase leading to a thermal peak, then a decrease phase. During the first phase (0 to approximately 0.5 h), the temperature increases slightly for all the samples, reflecting an initial thermal inertia linked to the progressive absorption of thermal energy and to the calorific capacity of the materials. Between 0.5 h and 2 h, a more marked increase is observed, with a relatively comparable slope for the three curves, indicating a quasi-stationary heating regime dominated by the heat conduction and accumulation mechanisms. However, slight differences appear : the C1 sample has slightly higher temperatures than those of C2 and CR, suggesting a better thermal conductivity or a higher storage capacity efficace. The third phase, centered around 2.5 h, corresponds to a pronounced thermal peak, with maximum temperatures of approximately 450 °C. for C1, 420 °C. for C2 and 380 °C. for CR. This maximum temperature difference highlights the influence of the physico-thermal properties of the materials (porosity, density, particle size or mineralogical composition) on the heat accumulation and restitution capacity. Finally, the decrease observed after the peak reflects the beginning of a cooling regime,

dominated by thermal losses by convection and radiation. The faster decay of the curve CR suggests a lower thermal inertia, while C1 retains a relatively higher temperature, indicating better thermal retention. Overall, these results show that, although the three materials are subjected to the same thermal conditions, their behaviors differ significantly in terms of maximum temperature reached and cooling kinetics. These differences are decisive for applications such as inserts or improved fireplaces, where a high temperature combined with good thermal retention is sought to optimize energy efficiency and heat recovery. Better thermal conductivity or a higher storage capacity efficace. The third phase, centered around 2.5 h, corresponds to a pronounced thermal peak, with maximum temperatures of approximately 450 °C. for C1, 420 °C. for C2 and 380 °C. for CR. This maximum temperature difference highlights the influence of the physico-thermal properties of the materials (porosity, density, particle size or mineralogical composition) on the heat accumulation and restitution capacity. Finally, the decrease observed after the peak reflects the beginning of a cooling regime, dominated by thermal losses by convection and radiation. The faster decay of the curve CR suggests a lower thermal inertia, while C1 retains a relatively higher temperature, indicating better thermal retention. Overall, these results show that, although the three materials are subjected to the same thermal conditions, their behaviors differ significantly in terms of maximum temperature reached and cooling kinetics. These differences are decisive for applications such as inserts or improved stove, where a high temperature combined with good thermal retention is sought to optimize energy efficiency and heat recovery.

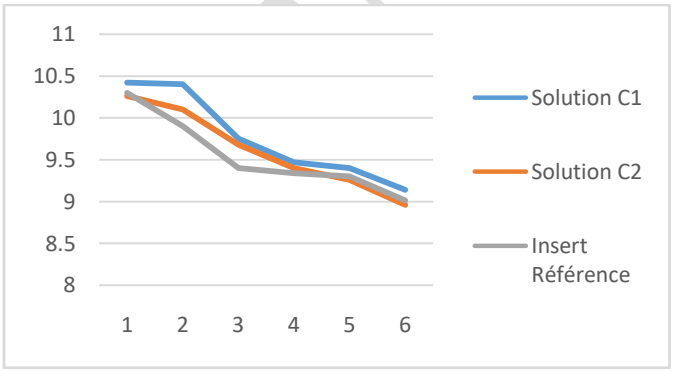

Fig 10: Curve of variation of the weight as a function of time

The Figure shows the evolution of the mass of the inserts C 1, C 2 and of the reference CR over time, over a period of approximately 2.5 hours. For all the formulations studied, the curves show a monotonous decrease in weight, reflecting a continuous process of mass loss, typically associated with the evaporation of free and bound water, as well as with the possible

decomposition of certain volatile phases under the effect of temperature. In the initial phase (0-0.5 h), a rapid loss of mass is observed for the three inserts, more marked for C1 and C2 than for the reference CR. This step conventionally corresponds to the elimination of the water physically adsorbed in the most accessible pores. The higher slope for C1 suggests a greater initial porosity or a higher water content, favoring a faster mass release. Conversely, the CR formulation has a more moderate decrease, indicating a probably denser structure or a particle size distribution limiting the diffusion of moisture.

Between 0.5 and 1.5 h, the curves tend to become less steep, reflecting a phase of relative stabilization of the rate of mass loss. This intermediate zone is generally attributed to the elimination of capillary and partially bound water, a process controlled by internal diffusion and the microstructure of the material [18]. It is observed that the insert C2 retains a slightly lower mass than that of C1, which can be interpreted as a better evacuation of internal moisture, potentially linked to a more favorable particle size or to a better connectivity of the pores.

At the end of the test (1.5-2.5 h), the three curves converge towards similar values, with a slightly higher final mass for C1, followed by CR, while C2 has the lowest residual mass. This convergence indicates the achievement of a quasi-hygroscopic equilibrium, where the major part of the volatile species has been eliminated. The lower residual mass of C2 suggests a lower content of volatile phases or water, which may constitute an advantage for thermal applications requiring increased dimensional and mass stability during repeated heating cycles [19].

Overall, the comparative analysis shows that the solutions C1 and C2 have a faster mass loss kinetics than the reference CR, reflecting notable microstructural differences induced by the formulation. Among the two solutions, C2 appears to be the most stable in the long term, with a lower final mass and more regular kinetics, which could be favorable for inserts intended for storage or thermal recovery applications, where repeatability and durability are essential criteria

4.Conclusion

This study highlighted the decisive influence of the particle size distribution on the heat transfer mechanisms and the heat storage capacity of ceramic inserts made by alkaline activation, with a view to reducing the firing temperature. The results show that the particle size strongly determines the final microstructure of the material, by acting on the

compactness, the porosity and the continuity of the alkalinally activated matrix, key parameters governing the thermal conductivity and the thermal inertia of the inserts.An optimized particle size distribution, combining fine and coarse fractions, promotes better reactivity during alkaline activation and effective densification at lower processing temperatures than those required for conventional ceramics. This microstructural structuring makes it possible to improve the heat transfer during the heating phase while ensuring an increased storage capacity and progressive heat recovery, despite the decrease in the cooking temperature. Conversely, uncontrolled particle size distributions lead either to excessive porosity, limiting thermal conductivity, or to structural heterogeneity likely to degrade thermal and mechanical performance. Alkaline activation thus appears as a relevant technological alternative to traditional high-temperature ceramic processes, by making it possible to obtain thermally efficient inserts at reduced firing temperatures. This approach contributes not only to improving the energy efficiency of the inserts, but also to reducing energy costs and the environmental footprint associated with their manufacture.

BIBLIOGRAPHIC REFERENCES

[1] J. Davidovits, "Geopolymers: new inorganic polymer materials", J. Therm. Anal., vol. 37, pp. 1633-1656, 1991 Journal of Thermal Analysis and Calometry

[2] "J. Davidovits, « The need to create a new technical language for the transfer of basic scientific information," in Transfer and exploitation of scientific and technical information, 1982, pp. 316-320 "

[3] "J. Wastiels, X. Wu, S. Faignet and G. Patfoort, "Mineral polymer based on fly ash", J. Resour.Manag. Technology., vol. 22, issue 3, pages 135-141, 1994 "

[4] "J. Davidovits, "Mineral polymer and manufacturing methods," U.S. Pat.No. 4,349,386 A, 1982"

[5] "H. Rahier, B. Van Mele and J. Wastiels, « Aluminosilicate glasses synthesized at low temperature-Part I - Low temperature reaction Stoichiometry and structure of a model compound", J. Mater. Sci., vol. 31, issue 1, pages 80-85, 1996 "

[6]."A_CHERKI-EL-IDRISSI J. Mater. Sci., vol. 3131, number 11, pages 80-85, 1996. [10] H. Rahier, B. Van Mele and J. Wastiels, "Aluminosilicate synthesized at low temperature July 24. 201 them.hal. Science9”

[7] "J. Davidovits and P. J. Davidovits,"30 Years of successes and failures in geopolymer applications market trends and potential breakthroughs" in Geopolymer Conference, 2002, pp. 1-16

[8] "Geopolymers: artificial rock geosynthesis and the results... 1 -2.1988. Page 16. Geopolymer 2002 Conference, October 28-29, 2002 ... "in Conference on Geopolymers, 2002, pp. 1-16”

[9] BELLION. Yes, GUIRAUD.R (1984) "Mineral Plan of the Republic of Senegal" 273p

[10] FAYE P. B. " 2012) "Treatment by alkaline activation of aluminum phosphate exploitation co-products for its use in road geotechnics, End of study thesis for obtaining the degree of design geologist engineer at the Institute of Earth Sciences (IST) of Cheikh Anta Diop University"

[11] PERACOD (2011) "Technical data sheet for the manufacture of Jambar wood and charcoal improved stoves. Program for the Promotion of Rural Electrification and Domestic Fuel Supply".

[12] GAYE A. "1996) "Determination of the optimal water content with a view to a compact road sand concrete. Thesis for the end of studies for obtaining the degree of design engineer at the Polytechnic School of Thies (EPT), 133p, July ".

[13] "Grim, 1968 ; Velde, 1995 ; Reed, 1995 Interactions natural clays tributaries dyers Tea Al Science".

[14] "WBT ISO-19867 Reference number ISO 19867-1 :2018(E)"

[15] "Incropera, F. P., DeWitt, D. P., Bergman, T. L., and Lavine, A. S. (2011). The results were published in 2011. Fundamentals of Heat and Mass Transfer. 7th ed., John Wiley and Sons"

(2012). Pollutant emissions and energy efficiency under controlled conditions for domestic biomass stoves. Environmental Science and Technology, 46(19), 10827-10834"

[16] "Bergman, TL, Lavine, AS, Incropera, FP and Dewitt, DP (2011) Fundamentals of heat and mass transfer. 7th Edition, John Wiley and Sons, Inc., 455-459”

[17] Çengel, AA, and Ghajar, AA (2020). The results of the study were published in 2015. Heat and mass transfer: Fundamentals and applications (6th ed.). McGraw-Hill Education"

[18] Introduction to ceramics. Front cover. W. David Kingery, H. K. Bowen and Donald R. Uhlmann. John Wiley & Sons, May 4, 1976-Technology and Engineering - 1056 pages.

[19] "Callister Jr., David G. Rethwisch. This is the first edition of the book. January 2018. 992 pages. Read an excerpt Index (PDF)Table of Contents (PDF)Chapter 01 (PDF). Product ... “